THE JOURNAL OF BIOLOGICAL CHEMISTRY VOL. 285, NO. 18, pp. 14062–14070, April 30, 2010

Allosteric Communication between cAMP Binding Sites in the RI Subunit of Protein Kinase A Revealed by NMR*[S]

Received for publication, January 26, 2010, and in revised form, February 27, 2010 Published, JBC Papers in Press, March 2, 2010, DOI 10.1074/jbc.M110.106666

In-Ja L. Byeon[‡], Khanh K. Dao[§], Jinwon Jung[‡], Jeffrey Keen[§], Ingar Leiros[¶], Stein O. Døskeland[§], Aurora Martinez[§1], and Angela M. Gronenborn[‡2]

From the [‡]Department of Structural Biology, University of Pittsburgh School of Medicine, Pittsburgh, Pennsylvania 15260, the [§]Department of Biomedicine, University of Bergen, Jonas Lies Vei 91, N-5009 Bergen, Norway, and the [¶]Norwegian Structural Biology Centre (Norstruct), Department of Chemistry, University of Tromsø, N-9037 Tromsø, Norway

The activation of protein kinase A involves the synergistic binding of cAMP to two cAMP binding sites on the inhibitory R subunit, causing release of the C subunit, which subsequently can carry out catalysis. We used NMR to structurally characterize in solution the RIα-(98–381) subunit, a construct comprising both cyclic nucleotide binding (CNB) domains, in the presence and absence of cAMP, and map the effects of cAMP binding at single residue resolution. Several conformationally disordered regions in free RIα become structured upon cAMP binding, including the interdomain αC:A and αC′:A helices that connect CNB domains A and B and are primary recognition sites for the C subunit. NMR titration experiments with cAMP, B site-selective 2-Cl-8-hexylamino-cAMP, and A site-selective N^6-monobutyryl-cAMP revealed that cyclic nucleotide binding to either the B or A site affected the interdomain helices. The NMR resonances of this interdomain region exhibited chemical shift changes upon ligand binding to a single site, either site B or A, with additional changes occurring upon binding to both sites. Such distinct, stepwise conformational changes in this region reflect the synergistic interplay between the two sites and may underlie the positive cooperativity of cAMP activation of the kinase. Furthermore, nucleotide binding to the A site also affected residues within the B domain. The present NMR study provides the first structural evidence of unidirectional allosteric communication between the sites. Trp^{262}, which lines the CNB A site but resides in the sequence of domain B, is an important structural determinant for intersite communication.

Protein kinase A (PKA)[3] is a primary receptor for cyclic adenosine monophosphate (cAMP) in eukaryotic cells (1, 2). In the absence of cAMP, the enzyme is an inactive, tetrameric holoenzyme complex, composed of two regulatory (R) and two catalytic (C) subunits (R_2C_2). The catalytic site of the C subunit is occluded by a short inhibitory sequence in the R subunit (residues 94–99 in bovine RIα) that connects the N-terminal dimerization domain to the two cyclic nucleotide binding (CNB) domains. Multiple contacts exist between the CNB domains and the C subunit. The enzyme is allosterically activated by cAMP (3, 4), whose binding to the R subunits causes dissociation of the C subunits from the holoenzyme complex, thereby rendering C catalytically active (5). Two CNB domains (A and B) are present in all four isoforms (RIα, RIβ, RIIα, and RIIβ) of mammalian PKA, and both need to be occupied by cAMP to achieve PKA dissociation under physiologically relevant conditions (for reviews, see Refs. 2 and 6). Newly transcribed R subunit (apoR) in the cell can complex with either cAMP or the C subunit of PKA. Binding of cAMP leads to a dramatically decreased affinity for the C subunit, whereas binding of the C subunit lowers the cAMP affinity by about 3 orders of magnitude (7), allowing the holoenzyme to respond to fluctuations in physiological cAMP concentrations (8, 9).

Comparing the crystal structures of RIα-(103–376) (numbering for bovine RIα) with cAMP bound in both the A and B domains (10) with the structure of RIα-(91–379) (R333K) complexed with the C subunit (4) revealed pronounced differences in the two CNB domains, in particular with respect to their relative positioning (Fig. 1). However, little is known about the structure of the ligand-free (apo) state of the R subunits. A truncated RIα (residues 119–244), comprising most of the A domain, has been investigated by NMR (11–13). Note, however, that this truncated form lacks not only the B domain but also the C-terminal end of the A domain, in particular the αC:A and αC′:A helices. These helices are at the junction between domains A and B and are important elements for interaction with the C subunit (4). Moreover, this region is conserved in all CAP-related eukaryotic cAMP binding proteins, as recently pointed out by Taylor *et al.* (14). For structural assessment of both the apo-state and the cAMP-bound state of RIα, and in order to reveal any allosteric communication between the domains, it is therefore necessary to investigate a protein with two intact CNB domains.

* This work was supported by grants from The Research Council of Norway (RCN), Helse-Vest, and the Norwegian Cancer Society (to A. M. and S. O. D.) and Commonwealth of Pennsylvania Grant SAP 4100026429 (to A. M. G.). NorStruct is supported by a grant from the National Program in Functional Genomics of the RCN.

[S] The on-line version of this article (available at http://www.jbc.org) contains supplemental Table S1 and Figs. S1 and S2.

[1] To whom correspondence may be addressed. Tel.: 47-55586427; Fax: 47-55586360; E-mail: aurora.martinez@biomed.uib.no.

[2] To whom correspondence may be addressed. Tel.: 412-648-9959; Fax: 412-648-9008; E-mail: amg100@pitt.edu.

[3] The abbreviations used are: PKA, cAMP-dependent protein kinase; 2-Cl-8-AH-cAMP, 2-chloro-8-hexylaminoadenosine-3′,5′-cyclic monophosphate; N^6-MB-cAMP, N^6-monobutyryladenosine-3′,5′-cyclic monophosphate; apo-form, cAMP-free R subunit (or in this work cAMP-free human RIα-(98–381)); C and R, catalytic and regulatory subunit, respectively, of PKA; CNB, cyclic nucleotide binding; DLS, dynamic light scattering; holo-form, the tetrameric form of PKA, including two catalytic (C) and two regulatory (R) subunits; PBC, phosphate-binding cassette; wt-RIα, wild-type full-length RIα; DTT, dithiothreitol.

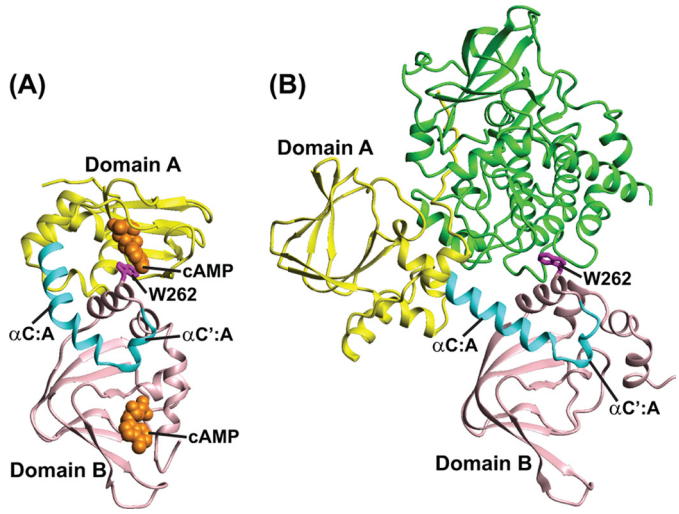

FIGURE 1. **Crystal structures of bovine RIα-(113–376) complexed with cAMP and of RIα-(91–379; R333K) complexed with the C subunit.** *A*, cAMP-bound bovine RIα-(113–376) structure (Protein Data Bank code 1RGS) (10); *B*, structure of bovine RIα-(91–379; R333K) complexed with the C subunit (Protein Data Bank code 2QCS) (4). The CNB A domain (up to residue 233) is shown in *yellow*, the αC:A and αC′:A helices in *cyan*, and the CNB B domain in *pink*. Residue Trp[262] (human numbering, corresponding to Trp[260] in bovine RIα) is shown in *magenta* in a *ball and stick representation*. In *B*, the C subunit is shown in *green*.

Here, we present an NMR study of RIα-(98–381), a construct that includes both CNB domains and the N-terminal region between the inhibitory sequence and the A domain, in the absence (apo-form) and presence of cAMP. We show that cAMP binding induces conformational stabilization of residues close to the binding sites as well as of regions that contact the C subunit of PKA. The conformational change of cAMP-ligated RIα in the area that interacts with the C subunit may explain why C binds to apoRIα with several orders of magnitude higher affinity than to cAMP-saturated RIα (15, 16). Titration of apoRIα with site-selective cAMP analogs permitted us to map the effects caused by single site occupancy at the amino acid level. Conformational changes observed for the αC:A helix, as well as the regions immediately preceding and following this helix, provided direct evidence for communication between the two binding sites and for additional structural effects that ensue only when both sites are occupied by cyclic nucleotide.

EXPERIMENTAL PROCEDURES

Mutagenesis, Expression, and Purification of RIα Proteins—Recombinant human wild-type full-length RIα (wt-RIα) and the C subunit of bovine PKA were obtained as described previously (17, 18). The DNA sequences corresponding to RIα-(92–381) and RIα-(98–381) were amplified by PCR from genomic DNA of human RIα (18) and cloned into pGEX-2T vectors (Amersham Biosciences). RIα-(98–381) was expressed as a Factor Xa-cleavable, N-terminal maltose-binding protein-tagged fusion protein. *Escherichia coli* BL21 (DE3) codon plus cells were used for protein production, induced at A_{600} 0.6–0.7 with 1 mM isopropyl 1-thio-β-D-galactopyranoside, and grown for an additional 7–10 h at 28 °C. Cells were harvested by centrifugation, resuspended in 20 mM sodium phosphate buffer (pH 7.3) containing 150 mM NaCl, 2 mM EDTA, 1% Triton X-100, 5 mM benzamidine, 1 mM DTT, 1 mM phenylmethylsulfonyl fluoride, and 2 μg/μl leupeptin and lyzed by passage through a French press. The fusion protein was purified by affinity chromatography on amylose resin (New England BioLabs), using 10 mM maltose in 20 mM Hepes buffer (pH 7.5) containing 0.2 M NaCl and 1 mM DTT for elution. Cleavage was carried out overnight at 4 °C with a Factor Xa/protein ratio of 1:240 (w/w). The cleaved protein was fractionated by gel filtration chromatography on a HiLoad Superdex 200 HR (1.6 × 60-cm) column (Amersham Biosciences) in 20 mM Hepes buffer (pH 7.0) containing 0.2 M NaCl and 1 mM DTT, followed by a final purification step using a prepacked RESOURCE™ Q column (Amersham Biosciences) and a linear NaCl gradient (0–0.5 M) in 20 mM Hepes buffer (pH 6.35) at a flow rate of 0.5 ml/min.

Removal of cAMP from the RIα Subunits—Purified recombinant RIα subunits (full-length and truncated forms) contain bound cAMP to various degrees, and fully saturated R subunits (R-cAMP$_2$) can be easily prepared by adding cAMP (60 mM) prior to the gel filtration step. In order to prepare cAMP-free proteins (apo-forms), an unfolding/refolding procedure was devised and optimized. Briefly, RIα-(98–381) and RIα-(92–381) proteins were incubated in 5 M urea in 10 mM potassium phosphate buffer (pH 7.4) containing 50 mM KCl, 1 mM EGTA for 5 h at 4 °C for partial unfolding. Complete removal of cAMP from the proteins was achieved by passage over a prepacked PD-10 column (GE Healthcare) and a couple of buffer exchanges using Amicon concentrators (Millipore, Billerica, MA). Refolding of the proteins was carried out by extensive dialysis against the same buffer without urea. Additional purification involved gel filtration on a HiLoad Superdex 200 HR (1.6 × 60-cm) column (Amersham Biosciences) for removal of soluble aggregates due to incomplete refolding. The absence of cAMP in the protein was verified by measuring the cAMP occupancy with [^{3}H]cAMP (Amersham Biosciences) as described previously (19).

Binding of cAMP Analogs to CNB Sites A and B of RIα-(98–381) and Full-length RIα— cAMP and cAMP analogs of 98% or better purity were obtained from Dr. G.-G. Genieser (BioLog Life Science Institute, Bremen, Germany). The relative affinity of each cAMP analog for the RIα subunit was estimated by competition experiments using protein-bound [^{3}H]cAMP by the validated ammonium sulfate precipitation method (17, 20).

Exchange of Bound cAMP at CNB Sites in Domains A and B of RIα and Kinase Activity—Nucleotide-free RIα, RIα-(92–381), or RIα-(98–381), each at 60 nM, were saturated with [^{3}H]cAMP (0.24 μM) by incubation for 30 min at 25 °C in 15 mM Hepes buffer (pH 7.2) containing 1 mM EDTA, 1 mg/ml bovine serum albumin, and 0.5 mM DTT. The exchange of the bound [^{3}H]cAMP with unlabeled cAMP was followed as described previously (3). In brief, exchange was initiated by rapidly mixing each of the above solutions with 20 volumes of buffer (15 mM Hepes buffer, pH 7.2) containing 3.2 M NaCl and excess (0.2 mM) unlabeled cAMP. Aliquots were removed after various periods of time during which exchange proceeded to determine the amount of [^{3}H]cAMP remaining bound. At such high NaCl concentrations, cAMP dissociates far more rapidly from site A than site B, permitting unambiguous evalu-

ation of whether labeled cAMP is bound to site A or site B (19). Kinase activity was measured by the phosphotransferase assay. The phosphorylation of heptapeptide substrate by PKA was determined essentially as described previously (21). The incubations were at 25 °C for 18 h with a 3.7 pM concentration of the catalytic subunit of PKA and various concentrations of the inhibitory full-length RIα and the non-inhibitory RIα-(98–381), in assay buffer (18 mM Hepes, pH 7.2, containing 0.1 mM heptapeptide substrate (Leu-Arg-Arg-Ala-Ser-Leu-Gly; Kemptide), 0.1 mM [γ-^{32}P]ATP, 2 mM $Mg(CH_3COO)_2$, 1 mM $NaHPO_4$, 0.4 mM EGTA, 0.1 mM EDTA, 130 mM KCl, 0.5 mM dithioerythritol, and 0.2 mg/ml each of bovine serum albumin and soybean trypsin inhibitor (0.2 mg/ml)).

Dynamic Light Scattering (DLS)—Solutions of RIα proteins in 10 mM potassium phosphate buffer, pH 7.4, 50 mM KCl (buffer A) were prepared, starting at ~0.74 mM and diluting 4-, 8-, and 32-fold, in the absence or the presence of cAMP. Samples were passed through a 0.22-μm Millipore filter, and 12 μl were loaded into a quartz cuvette and placed in the DynaPro LSR (Protein Solutions Inc.) DLS instrument with a temperature-controlled microsampler. 25 data acquisitions were collected for each solution at 22 °C. The data were analyzed using Dynamics version 6 (Protein Solutions) software to extract hydrodynamic radii, which are reported as the mean value for the dominant peak.

Preparation of U-^{2}H/^{13}C/^{15}N-Labeled Samples for NMR Studies—5 ml of starter cultures of *E. coli* expressing human RIα-(98–381) were grown in LB medium up to A_{600} ~0.4 and then centrifuged at 3000 rpm for 5 min. The cell pellet was added to 150 ml of ^{2}H/^{13}C/^{15}N-modified M9 medium (prepared with ^{13}C-perdeuterated glucose and ^{15}N-ammonium chloride in D_2O). Cells were grown at 37 °C up to A_{600} ~0.4, harvested by centrifugation, resuspended in 850 ml of ^{2}H/^{13}C/^{15}N-M9-D_2O-based medium, and grown again up to A_{600} ~0.4 at 37 °C for induction by 1 mM isopropyl 1-thio-β-D-galactopyranoside. Growth was continued at 25 °C for 14 h. Protein purification was carried out as described above for unlabeled RIα-(98–381).

NMR Spectroscopy—All NMR experiments were performed at 30 °C on Bruker Avance 900, 800, and 700 MHz spectrometers, equipped with 5-mm, triple resonance, and *z* axis gradient cryoprobes, using U-^{2}H/^{13}C/^{15}N-labeled RIα-(98–381) samples in 10 mM potassium phosphate buffer (pH 7.4) containing 50 mM KCl, 2 mM DTT, 0.02% sodium azide, and 7% $^{2}H_2O$. For backbone chemical shift assignments, two-dimensional ^{1}H-^{15}N TROSY-HSQC and three-dimensional TROSY-HNCACB, TROSY-HN(CO)CACB, TROSY-HNCA, and TROSY-HN(CO)CA experiments (22–24) were performed, ranging in protein concentration from 50 to 200 μM. To monitor binding to the A and B CNB domains, a 20 μM U-^{2}H/^{13}C/^{15}N-labeled RIα-(98–381) sample was titrated with aliquots of a 1 mM cAMP solution, and 50 μM U-^{2}H/^{13}C/^{15}N-labeled RIα-(98–381) samples were titrated with aliquots of 2 mM solutions of 2-Cl-8-AH-cAMP or N^6-MB-cAMP. A series of two-dimensional ^{1}H-^{15}N TROSY-HSQC spectra were acquired throughout the titration, following aliquot addition of each ligand. Titration isotherms were obtained by plotting bound RIα-(98–381) fractions *versus* molar ratios of ligand to RIα-(98–381) on six unambiguously assigned TROSY-HSQC resonances, three from each CNB domain. All spectra were processed with NMRPipe (25) and analyzed using NMRDraw and NMRView (26).

TABLE 1

Binding of cyclic nucleotides to the A- and B-sites in RIα(98–381) and wt-RIα

K_d values are reported relative to the K_d for cAMP (*i.e.* $K'_d = K_{d,cAMP}/K_{d,analog}$) for the different cyclic nucleotides. Mean values of three determinations are provided. The experimental error is ±15%.

Compound	RIα-(98–381)		wt-RIα	
	K'_d A	K'_d B	K'_d A	K'_d B
cAMP	1.0	1.0	1.0	1.0
N^6-MB-cAMP	3.8	0.070	3.7	0.071
2-Cl-cAMP	0.15	2.3	0.23	2.7
2-Cl-8-AH-cAMP	0.0031	1.7	0.0034	2.2
(S_p)-cAMPS	0.32	0.033	0.28	0.033
(R_p)-cAMPS	0.00046	0.0024	0.00043	0.0032

RESULTS

RIα-(98–381) Monomer Binds cAMP and cAMP Analogs Similar to wt-RIα—Due to its large molecular mass, dimeric full-length wt-RIα is not easily amenable to high resolution NMR studies. Monomeric RIα-(92–381) that lacks the dimerization/docking domain (residues 12–61) has been used extensively to mimic full-length RIα (2, 10). Our initial tests with human RIα-(92–381), however, revealed that the protein self-associates at concentrations above 0.1 mM, providing little prospect of obtaining high quality NMR data. A similar construct from bovine RI also formed homodimers through the N-terminal linker region (27). Fortunately, the removal of six additional residues rendered the protein, RIα-(98–381), monomeric at concentrations of 0.1 mM and above. Size exclusion chromatography of the cAMP-saturated-RIα-(98–381) protein revealed a single peak, and DLS measurements at 22 °C yielded an apparent hydrodynamic radius of 3.2–3.3 nm (supplemental Table S1), in agreement with dimensions extracted from the x-ray structure of the cAMP-bound RIα-(113–376) monomer (Protein Data Bank code 1RGS) (10). In contrast, apoRIα-(98–381) exhibited slight polydispersity, with an apparent radius of 3.8 nm. The hydrodynamic radius and polydispersity reverted readily back to the values for the cAMP-liganded protein after the nucleotide addition (supplemental Table S1), indicating that aggregation of apoRI is reversible upon cAMP binding.

RIα-(98–381) exhibited binding affinities similar to those of wt-RIα for cAMP and its analogs (Table 1) and the dissociation rate of bound cAMP is essentially identical between RIα-(98–381) and RIα-(92–381) and full-length RIα (supplemental Fig. S1*A*). The dissociation rate from site B of RIα is slowed 7-fold by site A occupancy (3, 19). The fact that a similar dissociation rate is found from site B in RIα-(98–381) and full-length RIα (supplemental Fig. S1*A*) suggests that the unidirectional effect of site A occupancy on the dissociation from site B (19) is unimpaired in the truncated RIα-(98–381). RIα-(98–381) also retained the ability to bind to the C subunit, as evidenced by its ability to competitively displace full-length RIα from its inhibitory complex with the C subunit (supplemental Fig. S1*B*). Therefore, we reasoned that RIα-(98–381) was a good candi-

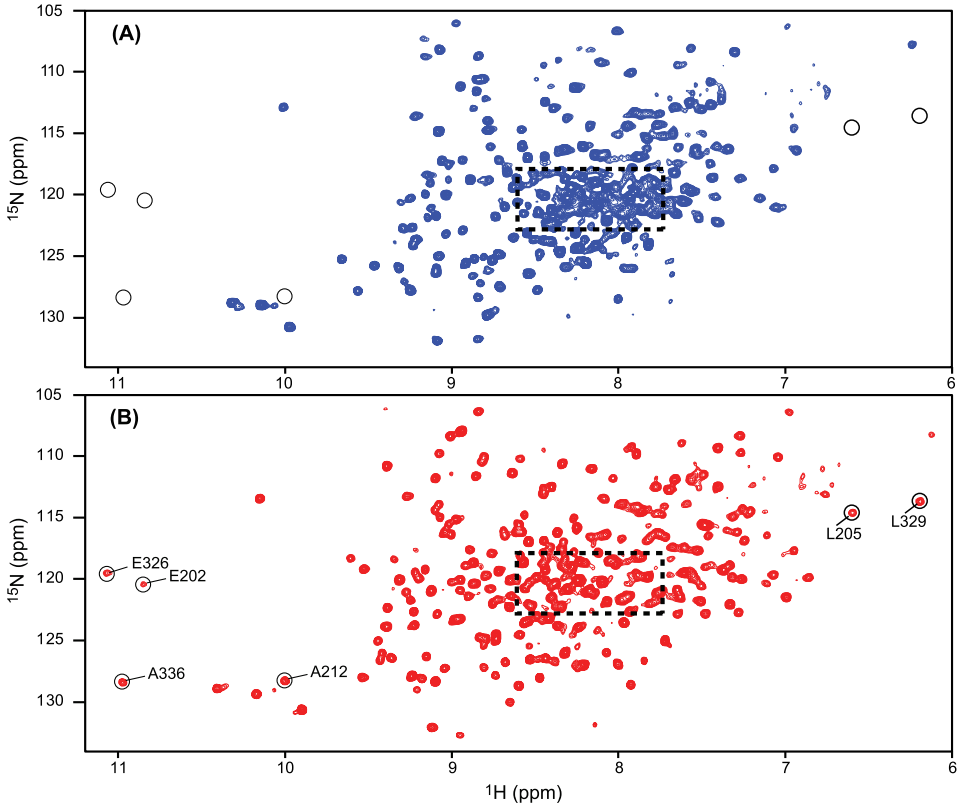

FIGURE 2. **^{1}H-^{15}N TROSY-HSQC spectra of RIα-(98–381).** The ^{1}H-^{15}N TROSY-HSQC spectra were recorded on 50 μM U-^{2}H/^{13}C/^{15}N-labeled RIα-(98–381) in the absence (*A*) and presence (*B*) of 200 μM cAMP. Several resonances that are only observed in the cAMP-bound RIα-(98–381) sample (*B*) are *circled* and *labeled* with residue name and number.

date for NMR studies that would allow us to obtain relevant data applicable to wt-RIα.

NMR Assignments of ApoRIα-(98–381) and cAMP-bound RIα-(98–381)—The ^{1}H-^{15}N TROSY-HSQC spectrum of cAMP-free apoRIα-(98–381) (Fig. 2*A*) is well dispersed (10.3–6.2 ppm for ^{1}H and 132–106 ppm for ^{15}N frequencies), indicative of a well folded protein. However, apoRIα-(98–381) had a tendency to slowly aggregate, resulting in about 50% NMR signal intensity loss after 1–2 weeks at 30 °C, in agreement with the aggregation behavior observed by DLS (supplemental Table S1). Similar instability/aggregation behavior has been reported for bovine RIα-(119–244) containing only one CNB domain (12). Fortunately, the addition of a trace amount of cAMP (about 15% of the cAMP-binding capacity of the protein) remarkably improved the long term stability of RIα-(98–381). NMR samples prepared in this manner were stable without detectable signal loss for more than 1 month, the time required for acquiring the full set of three-dimensional NMR experiments for complete backbone assignments, and exhibited essentially the same TROSY-HSQC spectrum as a completely cAMP-free sample, except for the presence of additional low intensity resonances from the cAMP-bound RIα-(98–381) fraction (supplemental Fig. S2). However, even with this sample, it was impossible to obtain complete assignments for the apoprotein because many of the resonances are weak and broad and reside in the severely crowded central spectral region exhibiting significant overlap (*dashed box* in Fig. 2*A*). Nevertheless, ~70% of all resonances were assigned, using perdeuterated protein samples, high sensitivity cryoprobes, and TROSY-type pulse sequences with ^{2}H decoupling (24).

NMR assignments of the backbone resonances of cAMP-bound RIα-(98–381) were carried out on a cAMP-saturated sample. Its ^{1}H-^{15}N TROSY-HSQC spectrum exhibited narrower line widths and better spectral dispersion than the spectrum of the apoprotein (Fig. 2*B*), permitting backbone assignments for 92% of the residues. The superior quality of the cAMP-saturated RIα-(98–381) spectrum is clearly apparent in the most crowded region (*dashed box*) and by the presence of resonances for residues such as Glu^{202}, Leu^{205}, and Ala^{212} in domain A, and Glu^{326}, Leu^{329}, and Ala^{336} in domain B that are absent in the apoprotein spectrum (*circled* in Fig. 2).

Structural Differences between cAMP-free and cAMP-saturated RIα-(98–381)—The secondary structures of apoRIα-(98–381) and cAMP-bound RIα-(98–381) were deduced from secondary chemical shifts of all assigned RIα residues (Fig. 3). As is well established (28), particular patterns of positive and negative secondary chemical shifts are reflective of helical and sheet conformations, respectively, and the observed shifts for cAMP-saturated RIα-(98–381) (Fig. 3*B*) agree with the α-helical and β-sheet regions in the x-ray structure of the bovine RIα-(92–379)-cAMP complex (Fig. 1*A*) (10). This implies that the overall structure in solution is similar to that observed in the crystal. On the other hand, several distinct differences were noted for the apoprotein. First, residues Glu^{202}–Tyr^{207}, Thr^{209}–Ala^{212}, and Glu^{326}–Ala^{336}, which belong to the phosphate-binding cassettes (PBCs), could only be assigned for the cAMP-bound protein (Figs. 2 and 3). Residues 202–207 and 326–331 constitute the αB′:A and αB′:B helices, respectively (Fig. 3), that stabilize cAMP binding by an N-terminal capping mechanism with the phosphate group (10, 12). Second, helices αC and αC′ at the C terminus of the A domain (αC:A and αC′:A) and helices αB and αC in the B domain (αB:B and αC:B) are also only present in the cAMP-bound protein (Fig. 3, *green shaded regions*). Note that the αC:A and αC′:A helices connect the A and B CNB domains, whereas helix αC:B is located at the C terminus of the entire RIα polypeptide chain and caps domain B upon cAMP binding (10, 29). Because a large proportion of resonances are broad and overlap in the "random coil" region of the ^{1}H-^{15}N TROSY-HSQC spectrum of the apoRI sample but not in the cAMP-bound sample (*dashed boxes* in Fig. 2, *A* and *B*), it is likely that the associated RIα segments comprising PBC residues and the αC helices are unstructured or ill structured in the apo-state,

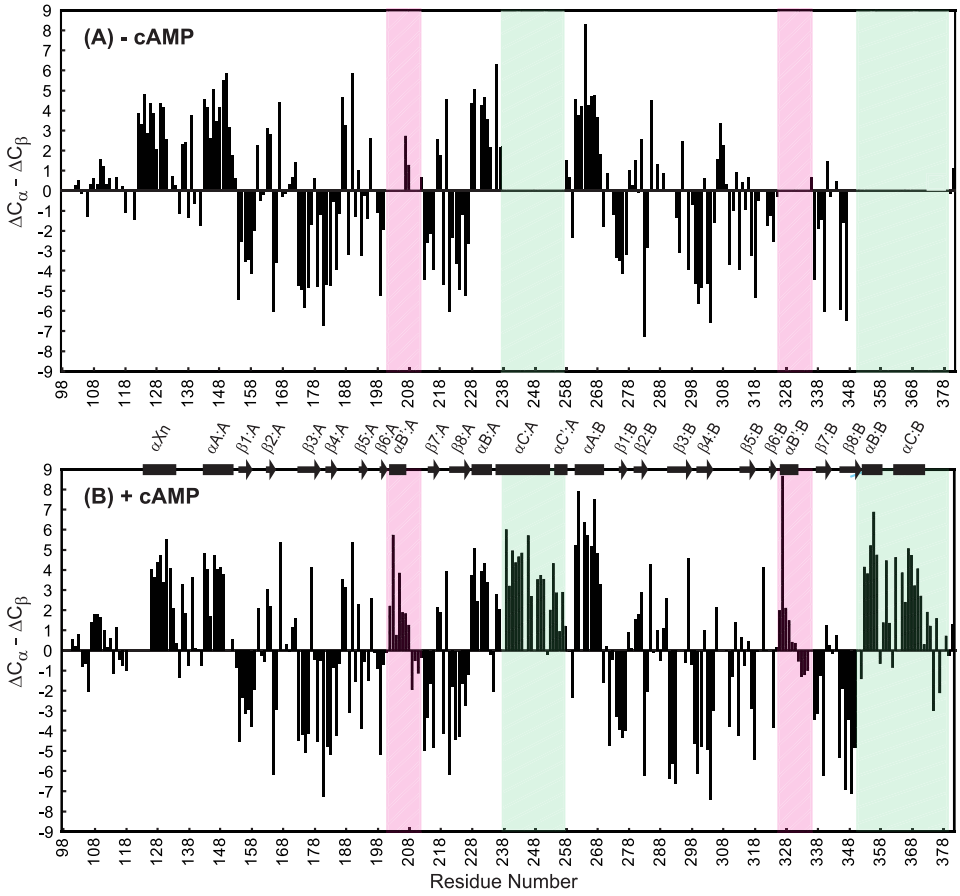

FIGURE 3. **C_α and C_β secondary chemical shift data for RIα-(98–381).** Secondary chemical shifts of the apoprotein (*A*) and cAMP-bound protein (*B*) are plotted *versus* residue number. The PBC regions are *boxed* in *pink*, and helices αC:A, αC′:A, αB:B, and αC:B are marked by *green boxes*. ΔC_α and ΔC_β are calculated by subtracting the C_α and C_β shifts from random coil values (46) for the residues whose chemical shifts were assigned unambiguously. α-Helices and β-strands present in the x-ray crystal structure of cAMP-bound bovine RIα-(92–379) (10) are depicted by *rectangles* and *arrows*, respectively.

exhibiting conformational averaging on an intermediate chemical shift (micro- to millisecond) time scale. This is in agreement with previous NMR studies of the apo form of the isolated A domain that reported a destabilization of the PBC region, evidenced by increased solvent exposure and dynamics upon the removal of cAMP (11, 12). Interestingly, all regions associated with high conformational flexibility in the apo-form are localized within the primary recognition area for the C subunit (4).

In addition to identifying the areas that are structured upon cAMP binding, the extent of any structural changes caused by ligand binding can be derived by analyzing the combined ^1H,^{15}N chemical shift changes for all assignable ^1H-^{15}N TROSY-HSQC resonances of apoRI and cAMP-bound RI (~60% of all residues; Fig. 4*A*). Binding of cAMP induced noticeable (>0.05 ppm) chemical shift changes for most resonances, with an average value of 0.15 ppm. In particular, resonances from residues in the loop between β2 and β3 in domain A showed substantial changes (>0.31; average change (0.15 ppm) plus one S.D. (0.16 ppm)) (Fig. 4*A*). This loop has recently been recognized as an important conserved area for the allosteric modulation of the CNB domains (14). It contains negatively charged residues (*e.g.* Asp^{172} in domain A) that position the conserved Arg in the PBC (14, 30). Other regions associated with substantial chemical shift changes are strands β6:A and β7:A and helices αB:A and αA:B. Note that these strands and helices, respectively, flank the PBC in domain A and the αC:A and αC′:A helices (Fig. 4*A*), whose regions are not assignable (visible) in the ^1H-^{15}N TROSY-HSQC spectrum of the apo-state protein (see above and Fig. 3*A*). Moreover, Trp^{262}, the residue for which cAMP binding induced the largest chemical shift change (1.2 ppm), is located in the αA:B helix (Fig. 4*A*). Finally, a stretch of residues (positions 103–118) in the N-terminal region of RIα-(98–381) that in full-length RI resides between the inhibitory sequence and the A CNB domain also exhibited noticeable (up to 0.3 ppm) chemical shift differences between the cAMP-free and cAMP-saturated protein. All chemical shift changes associated with cAMP binding are mapped onto the structure of RIα complexed with either cAMP (Fig. 4*B*) or the C subunit (Fig. 4*C*), with the position of Trp^{262} highlighted.

Binding of Site-selective Cyclic Nucleotide Analogs—The 2-Cl-8-AH-cAMP and N^6-MB-cAMP analogs show preferential binding for the B- and A- sites of CNB, respectively, of RIα-(98–381) (Table 1; see also Ref. 31). These analogs were used to study the effects of single site binding to RIα-(98–381). We first ascertained that the bound RIα-(98–381) chemical shifts (*red resonances* in the Tyr^{185} (*Y185*) panels) were similar for the protein fully saturated with cAMP (Fig. 5*A*), with the B analog (Fig. 5*C*), or with the A analog (Fig. 5*E*). This showed that these analogs induced very similar structural changes to cAMP.

Titration of RIα-(98–381) with the B site preferring analog 2-Cl-8-AH-cAMP up to a molar ratio of 1:1 revealed no spectral changes for residues located in the A domain (*e.g.* Val^{164}, Tyr^{185}, and Ala^{191}). In contrast, for B domain residues, such as Ala^{301}, Arg^{306}, and Gly^{319}, new resonances (*red*) appeared (Fig. 5, *C* and *D*), clearly confirming that this analog binds preferentially to the B site (Table 1). It is interesting to point out that resonances associated with residues in the PBC, the αB and αC helices in the B domain as well as the interdomain αC:A and αC′:A helices that were unassigned/undetected in the apoRI spectrum (Figs. 2 and 3), became readily visible upon the addition (1:0.5 ratio) of this B site analog (*e.g.* see Val^{253} (*V253*) in Fig. 5*C*). This indicates that nucleotide binding to site B alone is sufficient to induce structure in these regions. In particular, a distinct and interesting pattern was observed for residues located in helices αC:A and αC′:A. 2-Cl-8-AH-cAMP binding

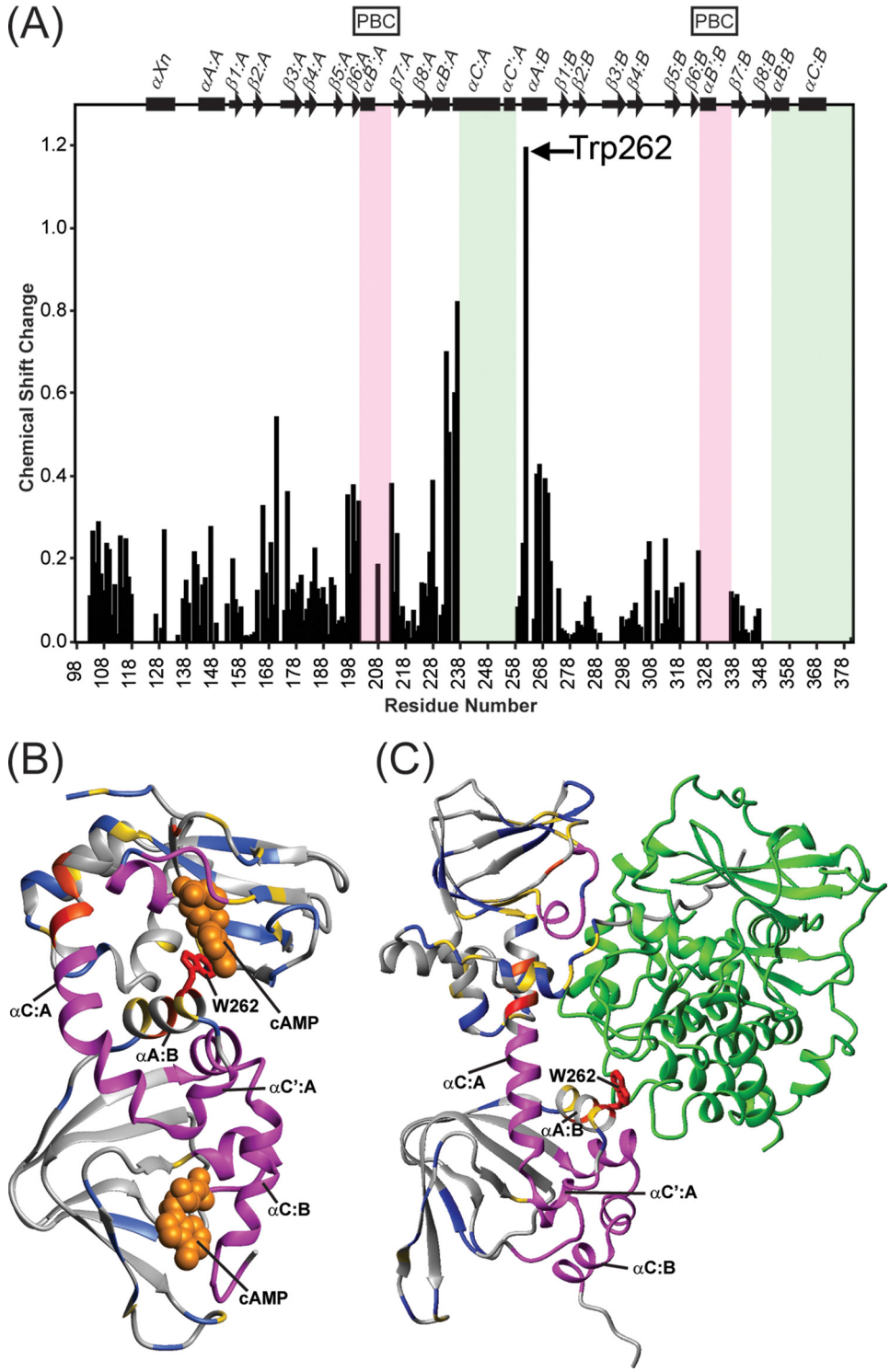

FIGURE 4. **Chemical shift changes in RIα-(98–381) upon cAMP binding.** *A*, the ^{1}H,^{15}N-combined chemical shift changes extracted from the ^{1}H-^{15}N TROSY-HSQC spectra were calculated using the square root of $\Delta\delta_{HN}^{2} + (\Delta\delta_{N} \times 0.1)^{2}$, where $\Delta\delta_{HN}$ and $\Delta\delta_{N}$ are the ^{1}HN and ^{15}N chemical shift differences, respectively, between the apo- and holoprotein. The PBC regions are *boxed* in *pink*, and the helix αC:A, αC′:A, αB:B, and αC:B regions are *boxed* in *green*. *B* and *C*, structural mapping of the chemical shift changes in the ^{1}H-^{15}N TROSY-HSQC spectrum of RIα-(98–381) induced by cAMP on the crystal structure of bovine RIα-(113–376) (Protein Data Bank code 1RGS) (*B*) and of bovine RIα-(91–379) (R333K) complexed with the C subunit (Protein Data Bank code 2QCS) (*C*). The *color scheme* used to differentiate the degree of chemical shift changes induced upon cAMP binding is as follows: *gray* for residues with <0.1 ppm, *blue* for those with 0.1–0.2 ppm, *gold* for those with 0.2–0.4 ppm, *reddish orange* for those with 0.4–0.8 ppm, and *red* for those with >0.8 ppm. In addition, the residues whose HSQC resonances are only detectable upon adding cAMP are *colored* in *magenta*. These residue are 202–207, 209–212, 239–258, 326–334, and 351–377 (human numbering). The Trp^{262} side chain is shown in *stick* representation and colored *red*. The *space-filling representation* of cAMP molecules is shown in *orange* in *B*, whereas the *ribbon representation* of subunit C is shown in *green* in *C*.

resulted in two types of bound resonances for Val^{253} (shown in Fig. 5*C*), Ser^{251}, and Leu^{259}. A new Val^{253} resonance (*purple* in Fig. 5*C*) becomes visible at the first addition of the nucleotide (1:0.5 ratio) and shows maximum intensity at a molar ratio of 1:1, when only the B site is occupied, whereas a second new resonance (*red* in Fig. 5*C*) gradually replaces the purple resonance at higher analog concentrations, when also the A site becomes occupied. Therefore, two distinct conformations of the αC:A and αC′:A helices can exist, one for the protein with cyclic nucleotide bound only in the B site and the other with ligand bound in both A- and B sites. Saturation of the A site induced no further changes of the bound resonances of the B domain residues (Fig. 5*C*). Therefore, binding of 2-Cl-8-AH-cAMP to site B is communicated to the αC:A and αC′:A helices, at the junction between the A and B domains, but not to domain A itself.

Titration with the A site preferring N^{6}-MB-cAMP up to molar ratio 1:0.6 resulted in essentially monosaturation of site A (Fig. 5, *E* and *F*). Interestingly, the titration data showed that binding to the A site alone caused widespread effects throughout the protein (Fig. 5, *E* and *F*). First and not surprisingly, spectral changes occurred for A domain residues like Gly^{180}, Tyr^{185}, and Gly^{198} (Fig. 5*E*), with gradual replacement of the free protein resonances (*blue*) by new ligand-bound resonances (*red*). Second, new (*purple*) resonances were also observed for B domain residues (Gly^{286}, Gly^{319}, and Ala^{341} in Fig. 5*E*). Moreover, the undetectable interdomain αC:A (Val^{253} in Fig. 5*E*) and αC′:A and C-terminal αC:B and αC:B helix residues became visible. Further addition of N^{6}-MB-cAMP resulted in the intensity increases of the A site bound resonances (*red*), reaching saturation at a molar ratio between 1:1.3 and 1:1.7. At the same point, resonances of ligand-free protein (*blue*) disappeared. The new (*purple*) B domain and αC:A helix

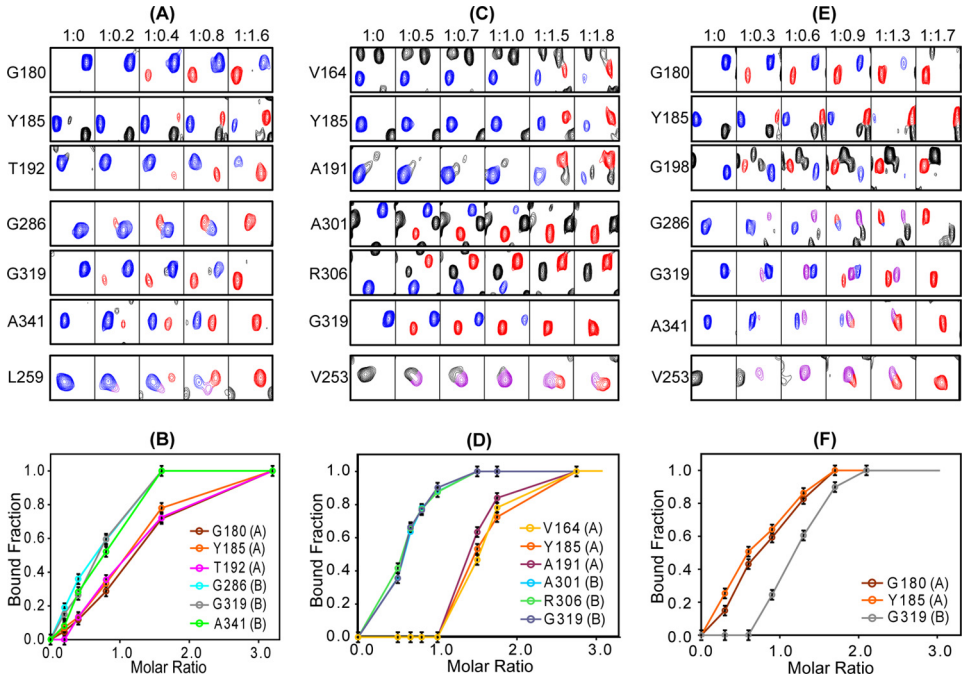

FIGURE 5. **Binding of cAMP and cyclic nucleotide analogs to RIα-(98–381).** Representative resonances from residues residing in the A and B domains as well as the linker helices (αC:A and αC′:A) were monitored throughout the titration with cAMP (*A* and *B*), 2-Cl-8-AH-cAMP (*C* and *D*), and N^6-MB-cAMP (*E* and *F*). *A*, *C*, and *E*, ligand-free RIα-(98–381) resonances are *colored* in *blue*, and ligand-bound resonances are shown in *red*. Resonances arising from intermediate bound conformations are shown in *purple* (see details under "Results"). The molar ratios for RIα-(98–381) and ligand are listed at the *top*. Titration curves for cAMP (*B*), 2-Cl-8-AH-cAMP (*D*), and N^6-MB-cAMP (*F*) are also shown where the bound fraction was obtained using the spectra in *A*, *C*, and *E*, respectively, by dividing the intensities of the bound resonances (*red*) by the sum of the intensities of the bound (*red*) and free (*blue*) resonances. The CNB domains A or B, to which the residues belong are indicated in *parenthesis* next to the residue identification in *B*, *D*, and *F*.

resonances exhibited their maximum intensities at a molar ratio of ~1:0.9, where other new resonances (*red*) started to appear, most likely due to actual ligand binding at the B site. The red resonances completely replaced the purple resonances at a molar ratio of 1:1.7. Therefore, they indeed are caused by ligand binding to the B domain, whereas the purple resonances belong to protein with ligand bound only in the A site.

In summary, our titration data demonstrate that ligand binding to the A site alone affects the conformation of the interdomain αC:A helix region as well as the B domain, providing unequivocal evidence for allosteric communication from the A domain to the B domain.

Titration of RIα-(98–382) with cAMP, the natural ligand (Fig. 5, *A* and *B*), revealed a slight B site preference, in accord with previous knowledge (7, 20). At a molar ratio of 1:0.2, spectral changes were only seen for B domain residues, such as Gly^{286}, Gly^{319}, and Ala^{341} (*red* in Fig. 5*A*), reflecting binding to the B site only. Importantly, amino acids that are located in the domain-connecting helices, such as Ser^{251}, Val^{253}, and Leu^{259} (shown in *purple* in Fig. 5*A*) also exhibited new resonances, similar to those seen with the B analog 2-Cl-8-AH-cAMP. For increasing molar ratios of cAMP/RIα-(98–382), new resonances (*red*) were also observed for A domain residues, and the Leu^{259} resonance of the B site saturated form (*purple*) is replaced by one for fully saturated (*red*) RIα-(98–382) (Fig. 5*A*).

In conclusion, residues in the αC:A and αC′:A helices that connect domains A and B and are critically involved in communicating with the catalytic subunit clearly experience an allosteric conformational change imparted by binding of either the natural ligand cAMP or cAMP analogs to either of the two sites and followed by complete conformational change upon full saturation to both sites. The observed distinct stepwise conformational change induced by single to double site binding may be the structural correlate of the positive cooperativity observed in the PKA holoenzyme by cAMP binding (4, 7).

DISCUSSION

Conformational Flexibility of ApoRIα, a Crucial Feature for Understanding PKA Regulation—The structural investigation of the tandem CNB domains of the R subunit of PKA in its apo-state (cAMP- and C-free) has been hampered by conformational dynamics and instability of the protein. Here, we investigated RIα-(98–381), which comprises both cAMP binding domains structurally by NMR. The critical feature for our ability to study the apo-form of RIα-(98–381) is the presence of trace amounts of cAMP, rendering the sample stable for extended NMR data collection, necessary for resonance assignment. However, titrations with cyclic nucleotides were performed starting from the nucleotide-free apo-state, allowing us to dissect and define the role of each binding site. It therefore was possible to detect nucleotide-specific effects for each binding site throughout the regulatory subunit, including the interdomain regions. The cAMP binding sites of domains A and B were intact in RIα-(98–381) because they behaved like those in wt-RIα (Table 1 and supplemental Fig. S1). The ability of the cAMP binding domains to interact with the C subunit of PKA appeared also to be intact, the slightly lower affinity for the C subunit of RIα-(98–381) compared with wt-RIα (supplemental Fig. S1*B*) being easily explained by the loss of the pseudosubstrate motif (residues 92–96), whose binding to C is controlled by peptide substrates rather than by cAMP (21).

ApoRIα binds to the C subunit of PKA several orders of magnitude tighter than cAMP-saturated RIα (15, 16). Comparison of conformational changes upon cAMP binding to RIα is therefore likely to provide important clues about the cAMP-mediated regulatory effects on the interaction with the catalytic domain. Crystal structures, NMR, small angle x-ray scattering analysis, and MD simulations of truncated forms of RIα either bound to cAMP or to the C subunit have already revealed that the R subunit is modular and dynamic and that a large conformational reorganization of RIα occurs upon binding to its partners (4, 10, 11, 32, 33) (see also Fig. 1). Our NMR studies con-

tribute to structurally map the areas for the conformational changes effected by cAMP binding, mainly the region N-terminal to domain A, the PBCs, and the αC:A, αC′:A, αB:B, and αC:B helices (Figs. 3 and 4, *A* and *B*), indicating that all intersubunit contacts identified in the crystal structure of the RIα-C complex (4) are severely perturbed by cAMP binding (Fig. 4*C*). These areas are characterized by a high degree of intrinsic disorder or conformational exchange in the apo-form and are structured upon binding, indicating that the high degree of flexibility of the R subunit may facilitate recognition of its functional partners (6, 14). Indeed, there is growing evidence that conformational dynamics is required for ligand recognition in numerous protein systems (34). Areas of intrinsic disorder provide the flexibility required to adopt interconverting conformations for proteins with several binding partners (34–37).

Interdomain Communication between the A and B Domains in RIα—The present NMR titration with cAMP and its analogs on RIα-(98–382) provides physical evidence for direct interdomain communication induced by cAMP binding, which has not been previously reported. The data demonstrate communication from the A site to the B site, but not vice versa, upon binding of cyclic nucleotide to one site. This important finding with regard to understanding allostery in the RI system may relate to the available kinetic data that show decreased dissociation and association rates of cAMP to site B after binding of the cyclic nucleotide to site A, without energetic coupling between the sites (19). Upon formation of the ternary complex of RI-cAMP and C, a similar acceleration of the cAMP dissociation rate from site B is observed when the A site becomes nonoccupied (3). This will contribute to a more rapid inactivation of PKA upon decrease of the intracellular cAMP levels.

Unlike in the free R subunit, the two cAMP binding sites in the R-C complex (PKA holoenzyme) are thermodynamically coupled, exhibiting positive cooperativity (4, 7, 38). The present study implicates the interdomain αC:A and αC′:A helices in mediating this effect. Residues residing in this region exhibit chemical shift changes upon cAMP bound to either site A or to site B that undergo further changes when both cAMP sites are occupied (Fig. 5). Previous mutational studies have already linked this region with cAMP binding to site A. For example, Glu^{202}, Leu^{205}, and Ile^{206} in the PBC, Asp^{172} (which interacts with the conserved Arg in the PBC), and the αC:A and αC':A helices are all sensitive to cAMP binding in the A site (14, 39–41). Previous NMR studies on R truncated at position 246 also revealed communication between A site binding and the αC:A helix (11, 12, 30, 42). However, the cumulative and sequential structural effect on the interdomain helices affected by binding of cAMP to both sites, as well as the communication of cAMP binding in the A site to the B domain, is observed here for the first time. A central residue in the A site to B site communication is Trp^{262} (Trp^{260} for bovine RIα), which is located at the beginning of the αA:B helix in the B domain. This Trp residue stacks with the adenine ring of cAMP bound in the A site (see Fig. 1), and its backbone HN resonance exhibits the largest chemical shift change upon cAMP binding (Fig. 4*A*). The important role of this Trp residue in allosteric communication is supported by extensive site-directed mutagenesis studies (4, 43, 44).

Functional Consequences of the Synergy between cAMP Binding to the Individual A and B Sites—It is known that cAMP binding to either site decreases the affinity between C and R in the PKA holocomplex several fold (7, 18, 45). However, only upon saturation of both sites does the affinity decrease enough to release C and thus cause activation under physiological conditions (18, 45). In addition, there is evidence for preferential binding to the B site over the A site for holoenzyme dissociation (16). This feature is related to the R-C holocomplex architecture because the binding site on the A domain is inaccessible until cAMP binds to domain B (4, 45). Here, we found that cAMP binds preferentially to the B domain in the isolated R subunit (or RIα-(98–381)), in perfect accord with previous results (7, 20). Moreover, the results show that both B site and A site binding alter the conformation of the αC:A and αC′:A helices (Fig. 5, *A–F*). However, only when both sites are occupied does the interdomain helical region adopt the final conformation of the cAMP-saturated state, in agreement with the observed synergistic interplay between sites A and B in PKA activation (18, 45).

In summary, the present NMR investigation on the N-terminally truncated human RIα-(98–381) uncovered pronounced and far reaching structural changes upon cAMP binding. Strikingly, all areas that undergo conformational changes upon cAMP binding to the apoR subunit of RIα involve recognition sites for the C subunit, observed in the crystal structure of the PKA holoenzyme. Moreover, site-specific occupancy of site A or site B allowed the detection of interdomain communication as well as allosteric communication between each cAMP binding site and the αC:A/αC′:A helices. This region, involved in intersite thermodynamic coupling (positive cooperativity) also resides in the R-C interface in the PKA holoenzyme, therefore directly linking nucleotide binding to activation.

Acknowledgments—We thank Dr. Jinwoo Ahn for useful discussions regarding protein expression and purification, Mike Delk for technical support regarding NMR instrumentation, Dr. Nils Åge Frøystein for support with the initial NMR investigations, and Gry Evjen for assistance with DLS experiments.

REFERENCES

1. Beavo, J. A., and Brunton, L. L. (2002) *Nat. Rev. Mol. Cell Biol.* **3,** 710–718
2. Taylor, S. S., Kim, C., Vigil, D., Haste, N. M., Yang, J., Wu, J., and Anand, G. S. (2005) *Biochim. Biophys. Acta* **1754,** 25–37
3. Houge, G., Steinberg, R. A., Ogreid, D., and Døskeland, S. O. (1990) *J. Biol. Chem.* **265,** 19507–19516
4. Kim, C., Cheng, C. Y., Saldanha, S. A., and Taylor, S. S. (2007) *Cell* **130,** 1032–1043
5. Rosen, O. M., and Erlichman, J. (1975) *J. Biol. Chem.* **250,** 7788–7794
6. Rehmann, H., Wittinghofer, A., and Bos, J. L. (2007) *Nat. Rev. Mol. Cell Biol.* **8,** 63–73
7. Dao, K. K., Teigen, K., Kopperud, R., Hodneland, E., Schwede, F., Christensen, A. E., Martinez, A., and Døskeland, S. O. (2006) *J. Biol. Chem.* **281,** 21500–21511
8. Eigenthaler, M., Nolte, C., Halbrügge, M., and Walter, U. (1992) *Eur. J. Biochem.* **205,** 471–481
9. Martin, B. R., Deerinck, T. J., Ellisman, M. H., Taylor, S. S., and Tsien, R. Y. (2007) *Chem. Biol.* **14,** 1031–1042
10. Su, Y., Dostmann, W. R., Herberg, F. W., Durick, K., Xuong, N. H., Ten Eyck, L., Taylor, S. S., and Varughese, K. I. (1995) *Science* **269,** 807–813

11. Das, R., Abu-Abed, M., and Melacini, G. (2006) *J. Am. Chem. Soc.* **128,** 8406–8407
12. Das, R., Esposito, V., Abu-Abed, M., Anand, G. S., Taylor, S. S., and Melacini, G. (2007) *Proc. Natl. Acad. Sci. U.S.A.* **104,** 93–98
13. Das, R., and Melacini, G. (2007) *J. Biol. Chem.* **282,** 581–593
14. Kornev, A. P., Taylor, S. S., and Ten Eyck, L. F. (2008) *PLoS Comput. Biol.* **4,** e1000056
15. Builder, S. E., Beavo, J. A., and Krebs, E. G. (1980) *J. Biol. Chem.* **255,** 3514–3519
16. Døskeland, S. O., Maronde, E., and Gjertsen, B. T. (1993) *Biochim. Biophys. Acta* **1178,** 249–258
17. Christensen, A. E., Selheim, F., de Rooij, J., Dremier, S., Schwede, F., Dao, K. K., Martinez, A., Maenhaut, C., Bos, J. L., Genieser, H. G., and Døskeland, S. O. (2003) *J. Biol. Chem.* **278,** 35394–35402
18. Kopperud, R., Christensen, A. E., Kjarland, E., Viste, K., Kleivdal, H., and Døskeland, S. O. (2002) *J. Biol. Chem.* **277,** 13443–13448
19. Døskeland, S. O., and Ogreid, D. (1984) *J. Biol. Chem.* **259,** 2291–2301
20. Schwede, F., Christensen, A., Liauw, S., Hippe, T., Kopperud, R., Jastorff, B., and Døskeland, S. O. (2000) *Biochemistry* **39,** 8803–8812
21. Viste, K., Kopperud, R. K., Christensen, A. E., and Døskeland, S. O. (2005) *J. Biol. Chem.* **280,** 13279–13284
22. Clore, G. M., and Gronenborn, A. M. (1998) *Trends Biotechnol.* **16,** 22–34
23. Bax, A., and Grzesiek, S. (1993) *Acc. Chem. Res.* **26,** 131–138
24. Salzmann, M., Wider, G., Pervushin, K., Senn, H., and Wüthrich, K. (1999) *J. Am. Chem. Soc.* **121,** 844–848
25. Delaglio, F., Grzesiek, S., Vuister, G. W., Zhu, G., Pfeifer, J., and Bax, A. (1995) *J. Biomol. NMR* **6,** 277–293
26. Johnson, B. A. (2004) *Methods Mol. Biol.* **278,** 313–352
27. Wu, J., Jones, J. M., Nguyen-Huu, X., Ten Eyck, L. F., and Taylor, S. S. (2004) *Biochemistry* **43,** 6620–6629
28. Spera, S., and Bax, A. (1991) *J. Am. Chem. Soc.* **113,** 5490–5492
29. Wu, J., Brown, S., Xuong, N. H., and Taylor, S. S. (2004) *Structure* **12,** 1057–1065
30. Abu-Abed, M., Das, R., Wang, L., and Melacini, G. (2007) *Proteins* **69,** 112–124
31. Christensen, A. E., and Doskeland, S. O. (2003) in *Handbook of Cell Signaling* (Bradshaw, R., and Dennis, E., eds) pp. 549–554, Academic Press, Inc., San Diego, CA
32. Cheng, C. Y., Yang, J., Taylor, S. S., and Blumenthal, D. K. (2009) *J. Biol. Chem.* **284,** 35916–35925
33. Gullingsrud, J., Kim, C., Taylor, S. S., and McCammon, J. A. (2006) *Structure* **14,** 141–149
34. Wright, P. E., and Dyson, H. J. (2009) *Curr. Opin. Struct. Biol.* **19,** 31–38
35. Uversky, V. N., Oldfield, C. J., and Dunker, A. K. (2005) *J. Mol. Recognit.* **18,** 343–384
36. Dyson, H. J., and Wright, P. E. (2005) *Nat. Rev. Mol. Cell Biol.* **6,** 197–208
37. Teilum, K., Olsen, J. G., and Kragelund, B. B. (2009) *Cell Mol. Life Sci.* **66,** 2231–2247
38. Ogreid, D., and Doskeland, S. O. (1982) *FEBS Lett.* **150,** 161–166
39. Ringheim, G. E., and Taylor, S. S. (1990) *J. Biol. Chem.* **265,** 19472–19478
40. Gibson, R. M., Ji-Buechler, Y., and Taylor, S. S. (1997) *J. Biol. Chem.* **272,** 16343–16350
41. Hahnefeld, C., Moll, D., Goette, M., and Herberg, F. W. (2005) *Biol. Chem.* **386,** 623–631
42. Das, R., Chowdhury, S., Mazhab-Jafari, M. T., Sildas, S., Selvaratnam, R., and Melacini, G. (2009) *J. Biol. Chem.* **284,** 23682–23696
43. Cànaves, J. M., Leon, D. A., and Taylor, S. S. (2000) *Biochemistry* **39,** 15022–15031
44. Gosse, M. E., Fleischmann, R., Marshall, M., Wang, N., Garges, S., and Gottesman, M. M. (1994) *Biochem. J.* **297,** 79–85
45. Herberg, F. W., Taylor, S. S., and Dostmann, W. R. (1996) *Biochemistry* **35,** 2934–2942
46. Wishart, D. S., and Sykes, B. D. (1994) *J. Biomol. NMR* **4,** 171–180